Available online at www.sciencedirect.com
SCIENCE DIRECT®
Journal of Chromatography A, 1051 (2004) 25–32
JOURNAL OF CHROMATOGRAPHY A
www.elsevier.com/locate/chroma

Heart-cutting two-dimensional electrophoresis in a single capillary

Hervé Cottet*, J.-P. Biron, Jacques Taillades

Laboratoire Organisation Moléculaire, Évolution et Matériaux Fluorés, UMR CNRS 5073, Université de Montpellier II, Case Courrier 17, Place Eugène Bataillon, 34095 Montpellier Cedex 5, France

Abstract

The possibility of performing two-dimensional capillary electrophoresis (2D-CE) separations in a single capillary was investigated. For this purpose, a fraction stemming from the first dimension of the separation was selected and isolated in the capillary by evacuating out of the capillary the other undesirable compounds. Next, the isolated fraction was submitted to a second separation medium that was introduced in the capillary by electroosmotic flow. The second separation medium was able to reach the isolated fraction since the solutes were migrating in counter-electroosmotic mode. Since only one fraction is submitted to the second dimension of the separation, this new methodology is closer to a heart-cutting approach than to a true comprehensive 2D separation. However, it has the advantage of not requiring any special coupling device between capillaries since the two dimensions of the separation are performed in the same capillary. In this work, a simple mixture of synthetic polymers taken as model compounds was separated according to: (i) the charge density by free solution CE in the first dimension, and (ii) the molar masses by CE in the presence of an entangled polymer solution in the second dimension. The different strategies that were investigated to isolate the fraction at the end of the first dimension are described in detail. The influence of important experimental parameters (capillary diameter, applied pressure for mobilizing the solutes, diffusion coefficients of the solutes) on the performances of the two-dimensional separations were studied. A careful attention was paid to the influence of these parameters on the efficiency of the separations. The experimental results demonstrate that heart-cutting 2D electrophoretic separations can be performed in a capillary format using a single capillary.

Keywords: Two-dimensional separations; Size and charge-based separations; Synthetic polymers; Entangled polymer solutions

1. Introduction

Samples are often complex in composition and can contain more than a hundred of components. The peak capacity of one-dimensional separations is often too low for handling such samples. Two-dimensional (2D) and, more generally, multi-dimensional separations offer the possibility to considerably increase the peak capacity [1,2]. Two criteria must be fulfilled for a separation to be considered as multidimensional [3]. First, the separations must be orthogonal each other. To be orthogonal, the mechanisms of separation must be based on different molecular characteristics. Second, the resolution obtained in one dimension of the separation must be preserved in the other dimensions.

Two-dimensional separations can be classified into two categories: the conventional comprehensive 2D separations and the heart-cutting 2D separations. Comprehensive two-dimensional separations are based on a frequent transfer of samples from one dimension to the second. Practically, this implies that the second dimension operates on a much faster scale than the first one. In heart-cutting 2D separations, only a fraction of the first dimension is subjected to the second dimension [1].

2D separations were first employed in a planar format. Earliest works involved 2D paper chromatography [4]. In 1975, O'Farrell [5] demonstrated that two-dimensional gel electrophoresis coupling isoelectric focusing with sodium dodecyl sulfate-polyacrylamide gel electrophoresis was able to resolve more than 1000 proteins. To make the 2D separations more quantitative, numerous 2D coupled-column systems, mainly based on chromatographic separation techniques, were developed [6]. The coupling of high perfor-

* Corresponding author. Tel.: +33 4 6714 3427; fax: +33 4 6763 1046.
E-mail address: hcottet@univ-montp2.fr (H. Cottet).

0021-9673/$ – see front matter © 2004 Elsevier B.V. All rights reserved.
doi:10.1016/j.chroma.2004.07.079

mance liquid chromatography (HPLC) with capillary zone electrophoresis (CZE) has been also investigated including the coupling of reversed phase liquid chromatography or size exclusion chromatography with CZE [1]. A review about the coupling of continuous separation techniques to capillary electrophoresis (CE), including the coupling of high-performance liquid chromatography or isotachophoresis to capillary electrophoresis, has been recently published [7]. Recent approaches including two-dimensional chromatographic or electrophoretic methods for the separation of peptides and proteins have also been reviewed [8]. Tanaka et al. [9] recently studied 2D-HPLC in a reversed-phase mode using monolithic silica columns for the second dimension separation. Nevertheless, very few works report the possibility of coupling together two CE methods. Mohan et al. recently published results concerning on-line capillary isoelectric focusing with transient capillary isotachophoresis coupled with capillary zone electrophoresis [10]. However, the coupling of two capillaries and the transfer of the fractions from the first to the second capillary are not simple tasks in a technical point of view. Ramsey and co-workers demonstrated the possibility to perform multidimensional electrophoresis using microchip electrophoresis [11].

In an attempt to overcome the inherent technical difficulties associated with the coupling of CE techniques, we have investigated the possibility of performing heart-cutting two-dimensional capillary electrophoresis (2D-CE) separations in a single capillary. For that, a fraction coming from the first dimension of the CE separation was selected and isolated in the capillary. Further, this fraction was submitted to a second separation medium, the latter being introduced in the capillary by electroosmotic flow. Indeed, we reported in a previous work the possibility of using electroosmotic pumping to fill capillaries with entangled polymer solutions even for highly viscous electrolytes [12]. In this work, the feasibility of this novel approach was first demonstrated using a simple mixture of synthetic polymers taken as model compounds. The first dimension of the separation consisted in the free solution CZE leading to a separation of the polymers according to their charge densities. The second dimension consisted in the size-based separation of the isolated fraction containing polyelectrolytes of different molar masses by CZE in the presence of an entangled polymer solution. The influence of important experimental parameters (capillary diameter, applied pressure for mobilizing the solutes, diffusion coefficients of the solutes) on the performances of the two-dimensional separations were investigated.

2. Materials and methods

2.1. Chemicals

Sodium tetraborate was from Fluka (Buchs, Switzerland). Hydroxyethyl cellulose (HEC; weight–average molar mass, M_w 250 × 10^3 g/mol) was from Aldrich (Steinheim, Germany). Deionized water was further purified with a Milli-Q-system from Millipore (Molsheim, France). One molar sodium hydroxide was from Prolabo (Briare-le-Canal, France).

2.2. Polymers

Standards of poly(styrene sulfonates) (PSSs, M_w 3.33 × 10^5 and 1.45 × 10^5 g/mol) were purchased from Polymer Standards Service (Mainz, Germany). The polydispersity indexes of both PSSs were below 1.2. Random copolymer (PAMAMPS) of acrylamide (90% in mol) and 2-acrylamido-2-methylpropanesulfonate (10% in mol) was synthesized by radical polymerization initiated by potassium persulfate and *N*,*N*,*N'*,*N'*-tetramethylethylenediamine according to the procedure described by McCormick and Chen [13]. The copolymer was purified by precipitation in absolute ethanol. The number average molecular weight of the PAMAMPS was evaluated (number average molar mass, M_n ∼3 × 10^5 g/mol) by size-exclusion chromatography using polyethyleneoxide standards for the calibration.

2.3. Capillary electrophoresis instrumentation

Capillary electrophoresis was carried out with a PACE MDQ Beckman Coulter (Fullerton, CA, USA) apparatus. Sample volumes were introduced hydrodynamically. The temperature of the capillary cassettes was maintained constant at 25 °C. Data were collected at 214 nm. Separation capillaries prepared from bare silica tubing were purchased from Composite Metal Services (Worcester, UK). Capillary dimensions were: 30 cm (20 cm to the detector) × 50, 25, 10 or 5 μm i.d. New capillaries were conditioned by performing the following washes: 1 M NaOH for 20 min and the electrolyte for 10 min. In between two runs the capillary was successively washed by water, 1 M NaOH and the electrolyte. The rinsing times were adapted according to the capillary i.d. in order to flush the capillary with at least two capillary volumes of each washing solution. Sample mixture 1 was prepared by dissolving the PSSs (0.5 g/L) and the PAMAMPS (5 g/L) in water. Sample mixture 2 was obtained by adding phtalate (0.5 g/L) to sample mixture 1. Sample mixture 3 was similar to sample mixture 2 but contained a higher concentrations in both PSSs (1 g/L). 0.05% (v/v) mesityl oxide was added to each sample mixtures as a neutral marker.

3. Results and discussion

To demonstrate the feasibility of heart-cutting 2D-CE separations in a single capillary, a mixture of three polyelectrolytes was first considered (sample mixture 1). The first component of the mixture was a random copolymer (compound A, PAMAMPS, M_n ∼3 × 10^5 g/mol) containing 90% (in mol) of a neutral monomer, acrylamide (AM), and 10% of a ionic monomer, sodium 2-(acrylamido)-2-

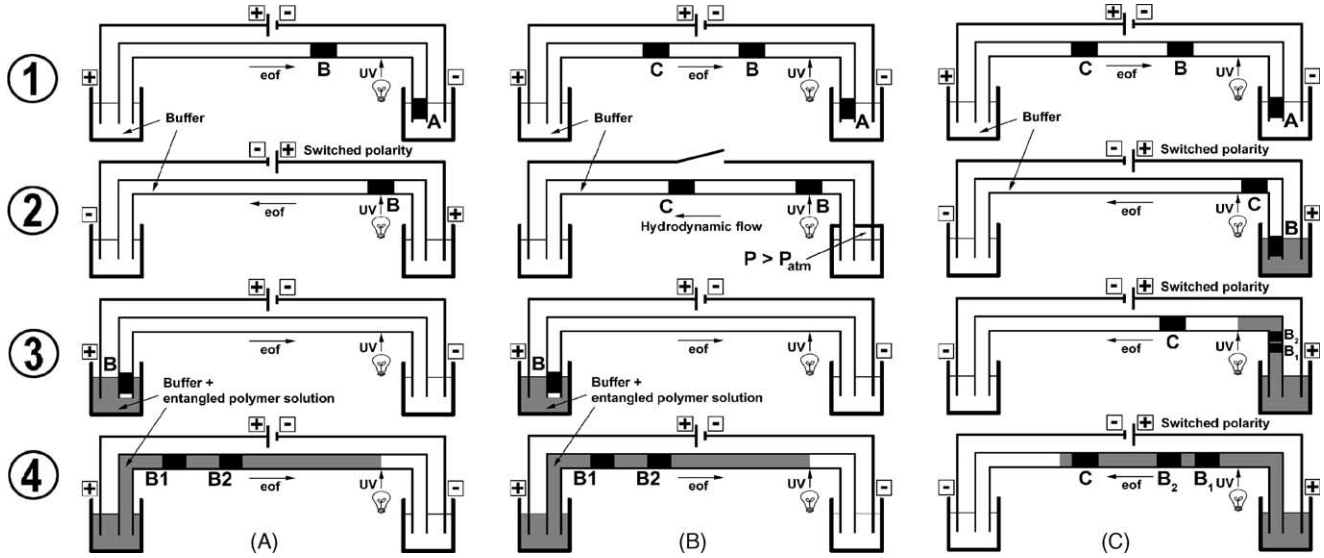

Fig. 1. Schematic representation of three different strategies (A–C) for performing heart-cutting 2D-CE separations in a single capillary. Each strategy is based on four key steps. Return of fraction B to the inlet end of the capillary by the application of a switched polarity (A) or a reverse hydrodynamic flow (B). Both fractions B and C are submitted to the second dimension of the separation (C). The electrolyte used for the second dimension of the separation is depicted in gray.

methylpropanesulfonate (AMPS). The mixture contained also two standards of PSS of different molar masses (compound B1, M_w 1.45 × 10^5 g/mol, and compound B2, M_w 3.33 × 10^5 g/mol). It is worth noting that this three components sample mixture can likely be separated using a single dimension CE separation under optimal conditions. However, since our main objective was to demonstrate on simple mixtures that heart-cutting 2D-CE can be performed in a single capillary, only 2D-CE approaches were investigated in this work. Three different strategies (A–C) are proposed to isolate the fraction of interest at the end of the first dimension (see Fig. 1). Each strategy is based on four key steps. In the first strategy (Fig. 1A), fraction B is isolated in the capillary by switching the voltage polarity (step 2), and is next subjected to the second dimension of the separation (steps 3 and 4). In the second strategy (Fig. 1B), fraction B is isolated in the capillary using an hydrodynamic flow. In the third strategy (Fig. 1C), both fractions B and C are subjected to the second dimension of the separation.

Fig. 2 shows the two-dimensional separation of the three aforementioned polyelectrolytes by CE in a single 50 μm i.d. fused silica capillary. The circled numerals in Fig. 2 refer to the four different key steps of the separation that are schematically depicted in Fig. 1A. Step 1 corresponds to the separation by free solution CE in a 80 mM borate buffer, pH 9.2. In these electrophoretic conditions, the polyelectrolytes were migrating in counter-electroosmotic mode and were separated according to their charge densities. Peak A corresponds to the 10% charged PAMAMPS and was thus detected before the peak assigned to the two comigrating PSSs of different molar masses (Peak B). In step 1, the separation voltage (+20 kV) was applied for 3 min until the undesirable peak A (PAMAMPS) was evacuated out of the capillary. Before proceeding to the second separation of the PSSs according to their molar masses, the polarity of the applied voltage was switched (step 2, −20 kV) for 2.75 min, so that fraction B could reach the inlet end of the capillary without being evacuated out of the capillary. Next, in step 3, the inlet vial was changed by an electrolyte containing an entangled polymer solution (0.5 g/100 mL HEC) in a 80 mM borate buffer. The

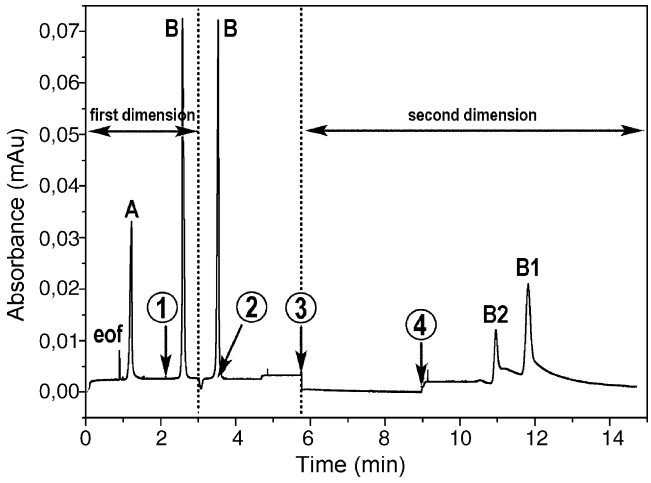

Fig. 2. Separation of three synthetic polymers by heart-cutting two-dimensional CE. Fused silica capillary, 20 cm (30 cm to the detector) × 50 μm i.d. Electrolyte: 80 mM borate buffer, pH 9.2 (first dimension); 80 mM borate buffer, pH 9.2 containing 0.5g/100 mL HEC (second dimension). Applied voltage: t = 0–3 min, +20 kV (first dimension); t = 3–5.75 min, −20 kV; t > 5.75 min, +6 kV (second dimension). Hydrodynamic injection of sample mixture 1: 0.3 psi, 3 s. UV detection at 214 nm. Temperature: 25 °C. Identification: A, PAMAMPS; B2, PSS (M_w 3.33 × 10^5 g/mol); B1, PSS (M_w 1.45 × 10^5 g/mol); B, B2 + B1; eof, electroosmotic flow. The status of the separation at four different steps (circled numerals) is schematically given in Fig. 1A.

second separation medium was then electroosmotically introduced in the capillary by the application of a relatively low positive voltage (+6 kV, step 3). Since the solutes (PSSs) were migrating in counter-electroosmotic mode, they were separated in this new electrolyte according to their molar masses (peaks B2 and B1 in Fig. 1, step 4 in Fig. 1A). The applied voltage was set at a lower value than that used in free solution CE to limit the detrimental effect of the biased reptation regime (orientation and stretching of the polymer solutes in the direction of the electric field) on the resolution of the size-based separation. The slight drop in the baseline at 9 min (Fig. 2, step 4) was due to the detection of the polymer solution (HEC).

In a second experiment, we tried to extend this methodology in a more general configuration where the fraction of interest in the first dimension of the separation (fraction B) was followed by other fraction(s) with smaller apparent mobilities (see step 1 in Fig. 1B). Experimentally, this situation was obtained by adding phtalate (compound C) to the sample mixture since its apparent mobility was found to be below that of the PSS in the 80 mM borate buffer. In step 2 of this scenario (Fig. 1B), the fraction B must reach back the inlet end of the capillary, and at the same time, the undesirable fraction C must be evacuated out of the capillary. This can be performed by the application of a pressure at the outlet end of the capillary resulting in an hydrodynamic flow directed from the outlet to the inlet end of the capillary. Indeed, the reversal in the polarity of the applied voltage from +20 to −20 kV, as previously described in step 2 of Fig. 1A, would induce a recombination of fractions B and C. The two other steps (steps 3 and 4 in Fig. 1B) were identical to those described in Fig. 1A and corresponded to the second dimension of the separation. Fig. 3 displays the electropherograms that were obtained in a 50 μm i.d. capillary according to the procedure depicted in Fig. 1B and for different durations (x in min) in the application of the hydrodynamic flow (step 2). The second electropherogram (x = 20 min) in Fig. 3 demonstrates that it was possible to evacuate fraction C out of the capillary while fraction B was kept inside the capillary. For x = 23 min, both phtalate (fraction C) and PSSs (fraction B) were evacuated out of the capillary, and thus, no peak was detected in the second dimension of the separation. Despite the very low pressure applied in step 2 (the lowest pressure that was permitted by the apparatus, i.e. 0.1 psi or 7.1 mbar), poor resolution (R_s = 0.8) between the two PSSs (B1 and B2) was observed in the second dimension of the separation (see Fig. 3, x = 20 min) in comparison with Fig. 2 (R_s = 3.4). This decrease in the resolution was attributed to peak broadening due to the laminar flow profile in contrast to the flat flow profile generated under electrophoresis conditions. Similar resolutions were obtained by applying a negative voltage of small intensity (−2 kV) in addition to the hydrodynamic flow in step 2 (electropherograms not shown). By this way, the total analysis time was decreased by a factor 1.33 due to the higher apparent velocities of the solutes in step 2. It is worth noting that the magnitude of the voltage (−2 kV) was sufficiently weak to avoid the recombination of fractions B and C.

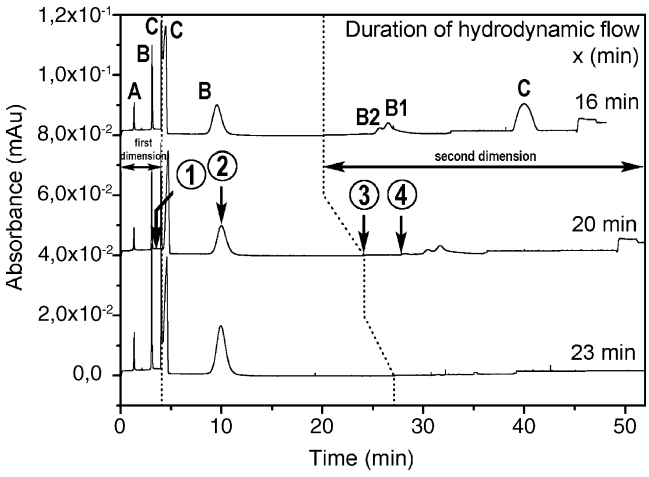

Fig. 3. Separation of four compounds by heart-cutting two-dimensional CE in a 50 μm i.d. capillary. Fused silica capillary, 20 cm (30 cm to the detector) × 50 μm i.d. First dimension: $0 < t < 4.1$ min, +20 kV. For $4.1 < t < 4.1 + x$ (min), 0.1 psi at the outlet end of the capillary. Second dimension: $4.1 + x < t$ (min), +6 kV. Hydrodynamic injection of sample mixture 2: 0.3 psi, 2 s. The status of the separation at four different steps (circled numerals) is schematically given in Fig. 1B. Other conditions and identification as in Fig. 2.

To minimize the loss in peak efficiency in step 2 (Fig. 1B), the value of the applied pressure was optimized as a function of the capillary i.d. For that, the heights equivalent to a theoretical plate H were measured for each of the four solutes under a pure hydrodynamic flow (no applied voltage) in a 30 cm (20 cm to the detector) × 25 μm i.d. capillary. The experimental H values were next plotted as a function of the applied pressure for all the solutes (Fig. 4). All these experimental values were fitted for each solute by non-linear regressions according to the following equation, taking the molecular diffusion coefficient D as the unknown parameter:

$$H = \frac{64\eta L D}{d_c^2}\frac{1}{P} + \frac{d_c^4}{3072\eta L D}P \quad (1)$$

where η is the viscosity of the electrolyte taken as that of water (0.89×10^{-3} Pa s at 25 °C), L the total capillary length, d_c the capillary diameter and P is the difference of pressure between both ends of the capillary. Eq. (1) is derived from the Van Deemter equation in the case of open tubular columns and for unretained solutes (for more details, see, for example [14]). H can also be written as a function of the linear velocity u of the electrolyte:

$$H = 2D\frac{1}{u} + \frac{d_c^2}{96D}u \quad (2)$$

As expected from Eqs. (1) and (2), the ascending portion of the curves in Fig. 4 was highly dependent on the diffusion coefficient. This portion was fairly flat for the phtalate compound (small molecule, large D value) while it was steep for the three polymer solutes (especially for the largest polymers,

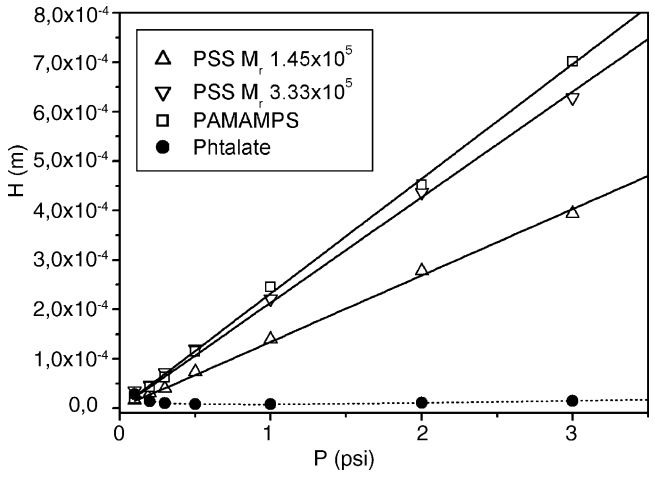

Fig. 4. Variations of the height equivalent to a theoretical plate as a function of the applied pressure for four solutes in a 25 μm i.d. capillary. The solutes were mobilized by a pure hydrodynamic flow, no voltage was applied. Fused silica capillary, 20 cm (30 cm to the detector) × 25 μm i.d. All measurements were performed in a 80 mM borate buffer. Hydrodynamic injection: 0.3 psi, 6 s. UV detection at 214 nm. Temperature: 25 °C. The lines were obtained by the non-linear regression of the experimental data using Eq. (1). The molecular diffusion coefficients derived from this non-linear curve fitting are gathered in Table 1.

i.e. PSS M_w 333 × 10^3 g/mol and PAMAMPS). Fig. 4 has also the merit to emphasize that very low pressures are needed to get reasonable peak efficiencies for polymer solutes, even on a 25 μm i.d. capillary. The D values obtained from the curve fitting in Fig. 4 were gathered in Table 1 and were compared with values derived from data of the literature. The molecular diffusion coefficient D of phtalate was estimated from the ionic mobility at infinite dilution [15] ($\mu^{0,\infty}$) using Eq. (3) based on the reasonable assumption that the electrophoretic frictional coefficient of such small molecule is similar to the hydrodynamic frictional coefficient [16]:

$$D = \frac{kT}{2e}\mu^{0,\infty} \tag{3}$$

where k is the Boltzmann constant, T the absolute temperature and e is the elementary charge. The D values for the PSS solutes were also estimated from data of literature using Eqs. (4) and (5):

$$R_g = \left(\frac{[\eta]M}{6^{3/2}\Phi}\right)^{1/3} \tag{4}$$

Eq. (4) is known as the Flory–Fox equation [17] and allowed us to estimate the PSS radius of gyration R_g from intrinsic viscosity $[\eta]$ (see, for example [18] for data of intrinsic viscosity on PSSs at different ionic strengths) and molecular mass M of the polymer. Φ is a constant equal to 1.4 × 10^{23} mol^{-1} for polyelectrolytes [19]. Next, the diffusion coefficient can be estimated from the Stoke–Einstein equation [20]:

$$D = \frac{kT}{6\pi\eta R_h} \approx \frac{kT}{9\pi\eta R_g} \tag{5}$$

where R_h is the hydrodynamic radius. In this latter equation a relationship between R_g and R_h was required. As a first approximation, we used the relation $R_h \approx 1.5R_g$ established for a gaussian chain (polymer in a θ solvent) [20]. The experimental D values derived from the curve fitting using Eq. (1) were in good agreement with the estimations from Eq. (3) (phtalate) and Eq. (5) (polymer solutes). The experimental values were found to be 3–5% higher than the estimated value from electrophoretic or viscosimetric data of the literature. These results prove that, under the experimental conditions of step 2 in Fig. 1B, Eq. (1) was suitable for describing the effect of pressure on the peak broadening.

As already mentioned, the optimum pressure value ($P_{opt,i}$) and the corresponding mobile phase velocity ($u_{opt,i}$), obtained by differentiating Eq. (1) with respect to the pressure and setting the result equal to zero, depends on the diffusion coefficient D_i of the solute i:

$$P_{opt,i} = 256\sqrt{3}\frac{\eta L D_i}{d_c^3} \tag{6}$$

$$u_{opt,i} = \frac{8\sqrt{3}D_i}{d_c} \tag{7}$$

Thus, it is impossible to set the pressure at a value that can minimize H for all the solutes when compounds of very different sizes such as small molecules and high molar-mass polymers are considered. Table 2 illustrates this difficulty by giving the optimal pressure for solutes of very different diffusion coefficients [PSS M_w 333 × 10^3 g/mol (B2) and phtalate (C)] in capillaries of different i.d. A compromise can however be obtained by setting the pressure at a value ($P_{opt,B2/C}$) for which the Van Deemter curves of the two solutes intercept, as illustrated by Fig. 5 for different capillary i.d. If $D_{B2} \ll D_C$,

Table 1
Comparison of experimental molecular diffusion coefficients (in m^2 s^{-1}) determined in this work with values calculated from data of the literature

	Phtalate (compound C)	PSS (M_r 145 × 10^3) (compound B1)	PSS (M_r 333 × 10^3) (compound B2)	PAMAMPS (compound A)
This work[a]	(7.06 ± 0.12) ×10^{-10} (r^2 = 0.994)	(2.38 ± 0.02) ×10^{-11} (r^2 = 0.999)	(1.51 ± 0.02) ×10^{-11} (r^2 = 0.999)	(1.37 ± 0.02) ×10^{-11} (r^2 = 0.999)
From data of the literature	6.8 × 10^{-10}[b]	2.30 × 10^{-11}[c]	1.45 × 10^{-11}[c]	–

[a] Values obtained from the non-linear curve fitting of the experimental data of Fig. 4 with Eq. (1).
[b] Value derived from the ionic mobility of phtalate at infinite dilution [15] (52.9 × 10^{-9} $m^2V^{-1}s^{-1}$) according to Eq. (3).
[c] Values calculated according to Eqs. (4) and (5) taking intrinsic viscosity data for PSS in water at 0.1 M ionic strength ($[\eta]$ = 1.68 × 10^{-4} $M^{0.68}$, $[\eta]$ in dL/g) [18].

Table 2
Optimal pressures (in psi) for minimizing the broadening effect of the hydrodynamic flow on a sample zone as a function of the capillary internal diameter and the nature of the solute(s)

	5	10	25	50
$P_{opt,B2}$ [a]	2.10	0.26	–[b]	–[b]
$P_{opt,C}$ [a]	95.6	12.0	0.76	0.1
$P_{opt,B2/C}$ [c]	14.3	1.80	0.11	–[b]

[a] The optimal pressure values were calculated using Eq. (6) with the experimental D values given in Table 1.
[b] The optimal pressure was below the minimal value that the apparatus could apply.
[c] The optimal pressure for the mixture B2/C was calculated using Eq. (8).

then $P_{opt,B2/C}$ is given by Eq. (8):

$$P_{opt,B2/C} = \sqrt{\frac{D_{B2}}{D_C - D_{B2}}} P_{opt,C} \quad (8)$$

Fig. 5 emphasizes that the use of capillaries with small i.d. allow the application of higher pressures resulting in higher linear velocities and should also lead to better peak efficiency. Of course, the reduction of the i.d. affects also the sensitivity of the detection.

Since in a 50 μm i.d. capillary, $P_{opt,B2/C}$ was below the lowest pressure P_{min} that the apparatus can produce (P_{min} = 0.1 psi), we tried to improve the two-dimensional separation by using a 25 μm i.d. capillary. Moreover, as previously described, a negative voltage of low intensity (−2 kV) was simultaneously applied with the optimal pressure $P_{opt,B2/C}$ (25 μm i.d.) ≈0.1 psi in step 2. The corresponding electropherograms are given in Fig. 5 for three different durations of step 2. In the upper electropherogram of Fig. 6, the duration (x = 25 min) of step 2 was not long enough for evacuating fraction C out of the capillary by the inlet end. On the contrary, for x = 28 min, the electropherogram in Fig. 6 shows that fraction C was completely evacuated of the capillary since peak C was not detected after peaks B1 and B2 during the second dimension of the separation. As exemplified in Fig. 6, good resolutions (R_s = 2.9 versus R_s = 0.8 in Fig. 3) were obtained for the separation of the two PSSs (B2 and B1) in the second dimension of the separation. The application of the negative voltage in step 2 may have also contribute to the reduction in the detrimental effect of the hydrodynamic flow on the peak broadening by diminishing the time required for fraction B to reach the inlet end of the capillary. Following the same approach, Fig. 7 displays the two-dimensional electropherograms that were obtained in capillaries of different i.d. The applied pressure in step 2 was set to a value close to the $P_{opt,B2/C}$ value (see last line in Table 2) excepted in the case of the 50 μm i.d. capillary where the pressure was set at the P_{min} value (0.1 psi). In addition to the hydrodynamic flow, a −2 kV voltage was simultaneously applied for diminishing the total analysis times. The peak symmetry, the resolution, the signal-to-noise ratio, as well as the total analysis time were dependent on the capillary i.d. In the 5 μm capillary, the peak asymmetry was critical and the signal to noise ratio was obviously very low. The peak asymmetry observed when using small internal diameter capillary was likely due to high electromigration dispersion (overloading of the capillary) since the polymer sample concentration was increased to improve the detection. The total analysis time in the 10 μm i.d. capillary was more than one and a half time shorter than in the 25 μm i.d. It appeared from the comparison of the second dimension of the separations as a function of the capillary i.d. that the 25 μm i.d. capillary was the best compromise in terms of resolution and signal to noise ratio.

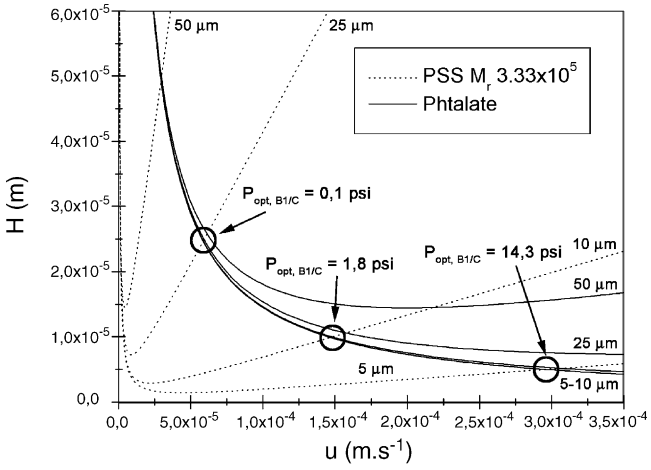

Fig. 5. Variations of the height equivalent to a theoretical plate as a function of linear velocity for PSS (M_w 333 × 10^3 g/mol, dotted line) and phtalate (plain line). The capillary i.d. is indicated on the graph for each curve. The curves were obtained using Eq. (2) and taking the molecular diffusion coefficients of the solutes given in Table 1. The optimal pressures to apply for a compromise in the dispersion of both two solutes are given on the graph for different internal diameters by the intersection of the plain and dotted curves.

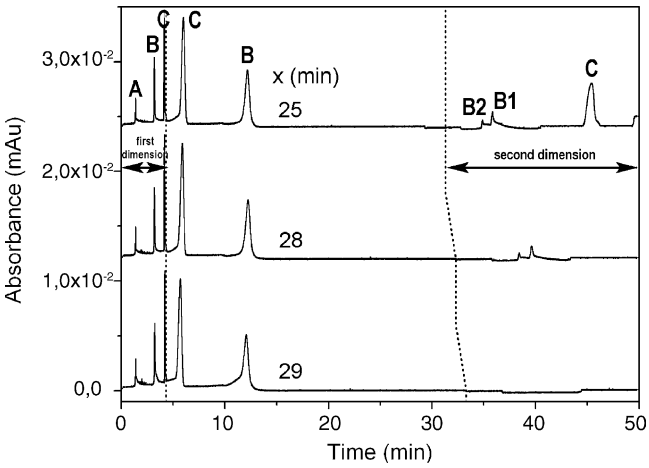

Fig. 6. Separation of four compounds by heart-cutting two-dimensional CE in a 25 μm i.d. capillary. Fused silica capillary, 20 cm (30 cm to the detector) × 25 μm i.d. First dimension: 0 < t <4.3 min, +20 kV. For 4.3 < t < 4.3 + x (min), 0.1 psi at the outlet end of the capillary and −2 kV. Second dimension: 4.3 + x < t (min), +6 kV. Hydrodynamic injection of sample mixture 2: 0.3 psi, 6 s. Other conditions and identification as in Fig. 2.

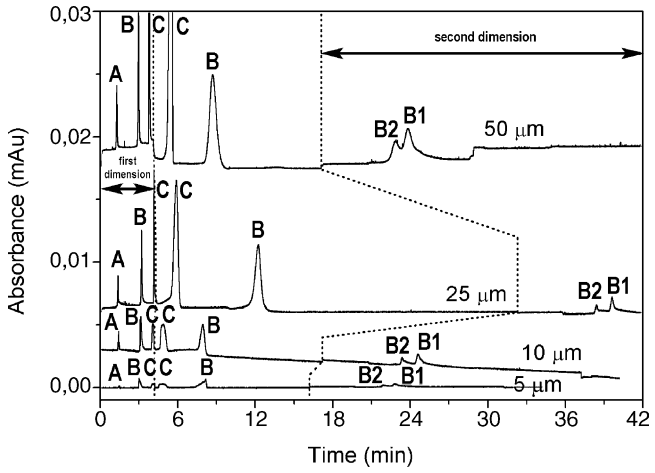

Fig. 7. Effect of the capillary i.d. on the separation of four compounds by heart-cutting two-dimensional CE. Fused silica capillary, 20 cm (30 cm to the detector). First dimension: +20 kV for $0 < t < 4.1$ min (50 μm i.d.), $0 < t < 4.3$ min (25 μm i.d.), $0 < t < 4.2$ min (10 and 5 μm i.d.). Application of −2 kV and a pressure of 0.1 psi (50 and 25 μm i.d.), 2 psi (10 μm i.d.), 25 psi (5 μm i.d.), at the outlet end of the capillary for $4.1 < t < 17.1$ min (50 μm i.d.), $4.3 < t < 32.3$ min (25 μm i.d.), $4.2 < t < 17.2$ min (10 μm i.d.), $4.2 < t < 16.2$ min (5 μm i.d.). Second dimension: +6 kV. Hydrodynamic injections: 0.3 psi, 2 s (50 μm i.d.); 0.3 psi, 6 s (25 μm i.d.); 1 psi, 20 s (10 μm i.d.); 20 psi, 30 s (5 μm i.d.). Sample mixtures 2 (50, 25, and 10 μm i.d.), sample mixture 3 (5 μm i.d.).

In the previous examples, a small fraction (one peak) of the first dimension was selected before being separated according to the second dimension. Fig. 1C depicts the different steps that were performed for submitting both fractions B and C to the second dimension of the separation. At the starting point of step 2, fraction A was already evacuated out of the capillary, fraction C was still in the capillary, while fraction B was close to the outlet end of the capillary. The entangled polymer solution was then electroosmotically introduced by the outlet end of the capillary by applying a −3 kV voltage. Relatively good resolution (R_s = 1.58) was obtained by this method (Fig. 8) even in the 50 μm i.d. capillary since there was no hydrodynamic flow in step 2 (Fig. 1C) that could induce peak broadening. However, when more than one fraction is submitted to the second dimension of the separation, components resolved in the first dimension can recombine in the second dimension.

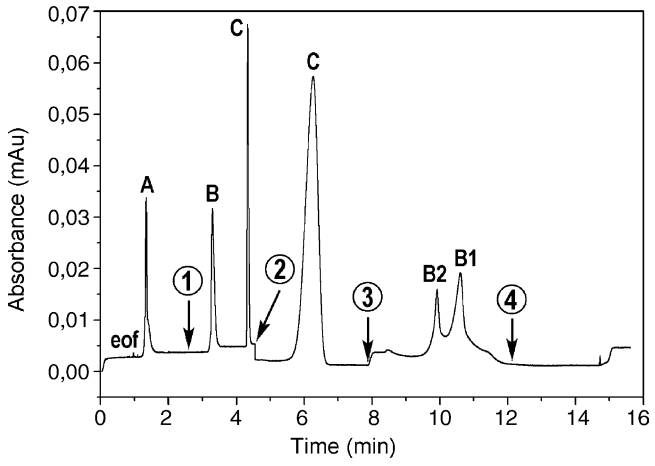

Fig. 8. Heart-cutting two-dimensional CE separation with selection of two fractions from the first dimension in a 50 μm i.d. capillary. Fused silica capillary, 20 cm (30 cm to the detector) × 50 μm i.d. Applied voltage: $0 < t < 4.55$ min, +20 kV (first dimension); $t > 4.55$ min, −3 kV (second dimension). The second separation medium was introduced at the outlet end of the capillary by electroosmotic flow. Both fractions B and C are submitted to the second dimension of the separation. Hydrodynamic injection: 0.3 psi, 3 s of sample mixture 2. Other conditions as in Fig. 2.The status of the separation at four different steps (circled numerals) is schematically given in Fig. 1C.

4. Conclusion

This work demonstrates that heart-cutting two-dimensional capillary electrophoresis can be performed in a single capillary using conventional apparatus. The proposed methodology does not require any special coupling device between capillaries since the two dimensions of the separation are performed in the same capillary. Due to the absence of coupling interface, there is potentially no loss of material between the two dimensions of the separation. The optimal capillary diameter as well as the optimal pressure for mobilizing the solutes, in terms of peak efficiency and in terms of sensitivity in the second dimension of the separation, depend on the molecular masses (or diffusion coefficient) of the solutes. When separating both small molecules and large solutes an internal diameter of 25 μm seems to be a good compromise. In this new methodology, there is one requirement concerning the second separation medium: it must be able to enter in the capillary with a higher apparent velocity than that of the isolated solutes. A simple way to fulfill this requirement is to perform the second dimension of the separation in counter-electroosmotic mode. This implies the existence of a cathodic electroosmotic flow for the separation of anions and an anodic (reversed) electroosmotic flow for the separation of cations.

References

[1] T.F. Hooker, D.J. Jeffery, J.W. Jorgenson, in: M.G. Khaledi (Ed.), High Performance Capillary Electrophoresis. Chemical Analysis Series, vol. 146, Wiley, New York, 1998, p. 581.
[2] Y. Shen, R.D. Smith, Electrophoresis 23 (2002) 3106.
[3] J.C. Giddings, J. High Resolut. Chromatogr. Commun. 10 (1987) 319.
[4] R. Consden, A.H. Gordon, A.J.P. Martin, Biochem. J. 38 (1944) 244.
[5] P.H. O'Farrell, J. Biol. Chem. 250 (1975) 4007.
[6] H.J. Cortes (Ed.), Multidimensional Chromatography: Techniques and Applications. Chromatographic Science Series, vol. 50, Marcel Dekker, New York, 1990.
[7] M. Valcarcel, L. Arce, A. Rios, J. Chromatogr. A 924 (2001) 3.
[8] H.J. Issaq, T.P. Conrads, G.M. Janini, T.D. Veenstra, Electrophoresis 23 (2002) 3048.
[9] N. Tanaka, H. Kinura, D. Tokuda, K. Hosoya, T. Ikegami, N. Ishizuka, H. Minakuchi, K. Nakanishi, Y. Shintani, M. Furuno, K. Cabrera, Anal. Chem. 76 (2004) 1273.

[10] D. Mohan, C.S. Lee, Electrophoresis 23 (2002) 3160.
[11] R.D. Rocklin, R.S. Ramsey, J.M. Ramsey, Anal. Chem. 72 (2000) 5244.
[12] H. Cottet, P. Gareil, J.-L. Viovy, Electrophoresis 19 (1998) 2151.
[13] C.L. McCormick, G.S. Chen, J. Polym. Sci. Polym. Chem. Ed. 20 (1982) 817.
[14] C.F. Poole, S.K. Poole, Chromatography Today, Elsevier, Amsterdam, 1991.
[15] H. Cottet, P. Gareil, Electrophoresis 21 (2000) 1493.
[16] P.D. Grossman, J.C. Colburn, H.H. Lauer, Anal. Biochem. 179 (1989) 28.
[17] S.F. Sun, Physical Chemistry of Macromolecules, Wiley-Interscience, New York, 1994.
[18] M. Tricot, Macromolecules 17 (1983) 1698.
[19] P.D. Grossman, J.C. Colburn, Capillary Electrophoresis: Theory and Practice, Academic Press, San Diego CA, 1992.
[20] W. Burchard, Solution Properties of Branched Macromolecules, in: Advances in Polymer Science, vol. 143, Springer, Berlin Heidelberg, 1999.